Compact, Wideband, Circularly Polarized, Inductive Grid-Array Metasurface Antenna

Qingli Lin[1], and Ming-Chun Tang[1]
[1] School of Microelectronics and Communication Engineering
Chongqing University
Chongqing, China
tangmingchun@cqu.edu.cn

Richard W. Ziolkowski[2]
[2] Global Big Data Technologies Centre
University of Technology Sydney
Ultimo NSW 2007, Australia
richard.ziolkowski@uts.edu.au

***Abstract* — A compact, wideband, circularly polarized (CP) dipole antenna is presented. The antenna consists of a directly driven, crossed Egyptian axe dipole (EAD) antenna stacked seamlessly in parallel with an inductive parasitic grid array metasurface within a circular package. The grid array structure is introduced to collaborate with the EAD antenna in producing overlapping resonances to achieve wideband CP radiation. The simulated impedance bandwidth, where $|S_{11}| < -10$ dB, is from 1.58 to 2.06 GHz (26.3%). The 3-dB AR bandwidth is from 1.67 to 2.08 GHz (21.8%). The consequent overlapping bandwidth is from 1.67 to 2.06 GHz (20.9%). The total dimensions of this very compact, low profile antenna are $\pi\times(0.19\lambda_0)^2\times0.0014\lambda_0 = 1.59\times10^{-4}\ \lambda_0^3$, where λ_0 is the wavelength of the lower bound frequency, 1.67 GHz. Moreover, the antenna radiates bidirectional electromagnetic fields with high radiation efficiency across the entire overlapping bandwidth.**

Keywords—Circularly polarized (CP), Egyptian axe dipole (EAD), grid array metasurface, near field resonant parasitic (NFRP), wideband.

I. Introduction

With the continuing expansion of wireless communication systems and the desired for highly compact devices, the room available on mobile platforms for their antenna systems has become more and more limited. This is particularly true in recent years with the rapid development of fifth-generation (5G) wireless systems. In a similar context, circularly polarized (CP) antennas are attracting more and more attention. They have many advantageous performance characteristics, including the reduction of multipath effects and polarization adaptation losses, while not having any additional considerations of the orientation of the transmitting and receiving antennas [1], [2]. Several types of compact CP antennas have been introduced to address the issues associated with space-limited wireless communication platforms. Examples include crossed-dipole CP antennas [3], [4] and microstrip patch CP antennas [5], [6]. Nevertheless, they are not easily modified for or adapted to broadband operations. As a result, the demand for compact CP antennas with broad bandwidths and high efficiencies has significantly increased.

In this paper, a compact, wide bandwidth, inductive grid array metasurface CP antenna is presented. It is composed of a crossed Egyptian axe dipole (EAD) antenna and a rectangular inductive grid array structure. It is a simple structure that is easily fabricated. The antenna radiates bi-directional CP electromagnetic waves with symmetric radiation patterns and high radiation efficiency across its entire operational bandwidth.

II. Antenna Design

A. Antenna Configuration

Fig. 1 presents the configuration and the elements of the developed compact, wideband CP antenna. This CP antenna evolved from our linearly polarized (LP) grid-array metasurface antenna reported in [7]. It consists of a directly driven crossed EAD antenna [8], [9] integrated with an inductive grid array metasurface structure. These elements are printed, respectively, on the upper and lower surfaces of a Rogers Duroid™ 5880 metal-clad substrate with relative dielectric constant $\varepsilon_r = 2.2$, loss tangent $\tan\delta = 0.0009$, and copper cladding thickness $H_1 = 0.017$ mm. The thickness of the substrate is $H_2 = 0.254$ mm. The antenna is fed by a 50-Ω coaxial line whose inner and outer conductors are directly connected to the two arms of the crossed EAD. The specific values of the design parameters of this CP antenna indicated in Fig. 1 are listed in Table I.

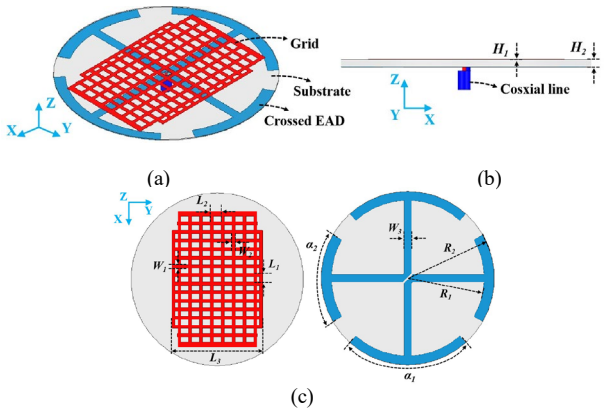

Fig. 1 The configuration, elements and design parameters of the developed wideband CP grid array antenna. (a) 3-D isometric view. (b) Side view. (c) Views of the upper and lower surfaces of the substrate.

TABLE I

OPTIMIZED DESIGN PARAMETERS OF THE DEVELOPED WIDEBAND CP GRID ARRAY ANTENNA (DIMENSIONS IN MILLIMETERS)

$H_1 = 0.017$	$H_2 = 0.254$	$L_1 = 3.48$	$L_2 = 3.3$	$L_3 = 36.64$
$W_1 = 1.28$	$W_2 = 1.16$	$W_3 = 2.9$	$R_1 = 31.2$	$R_2 = 35$
$\alpha_1 = 84.0°$	$\alpha_2 = 60.0°$	*NULL*		

B. *Surface Current Distributions*

To illustrate the CP behavior of the developed antenna, the surface current distributions on the crossed EAD and grid structure over one period in time at 1.83 GHz are shown in Fig. 2. They are highlighted with the additional blue and purple arrows, respectively. As demonstrated in the figure, the dominant currents on the grid structure, as well as those on the EAD, rotate clockwise over one period. Thus, they realize a left-handed circular polarization (LHCP) operation. Note that there is a 45° phase delay between the crossed EAD and the grid structure that facilitates this circular behavior.

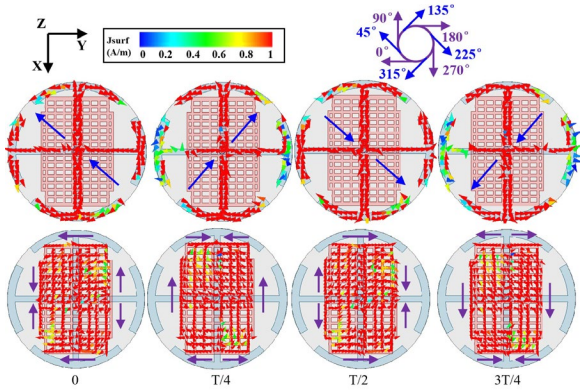

Fig. 2 Surface current distributions on the crossed EAD and the grid structure of the developed wideband CP antenna at 1.83 GHz over one time period T.

III. SIMULATED RESULTS

The simulated reflection coefficient, i.e., $|S_{11}|$ values, and the axial ratio (AR) curves as a function with the source frequency of the optimized antenna are shown in Fig. 3. The –10-dB impedance bandwidth is from 1.58 to 2.06 GHz which gives a fractional bandwidth of 26.3%. The 3-dB AR bandwidth is from 1.67 to 2.08 GHz with the corresponding fractional bandwidth being 21.8%. Consequently, the simulated overlapping operational bandwidth covers 390 MHz from 1.67 to 2.06 GHz. The corresponding fractional bandwidth is thus a high 20.9%.

The simulated realized gain and radiation efficiency values are plotted in Fig. 4. The simulated realized gain values are maintained around the peak of 2.2 dBi with a gain fluctuation that is within only 0.2 dB over the entire operational bandwidth. Moreover, the simulated radiation efficiencies values are larger than 89% over it. The 2-D normalized realized gain patterns at the selected (minimum $|S_{11}|$ value within the bandwidth) operating frequency, 1.83 GHz, are plotted in Fig. 5. The antenna radiates a bi-directional electromagnetic wave with symmetric radiation patterns. In particular, the antenna radiates LHCP fields in the forward broadside and right-handed circular polarization (RHCP) in the backward direction.

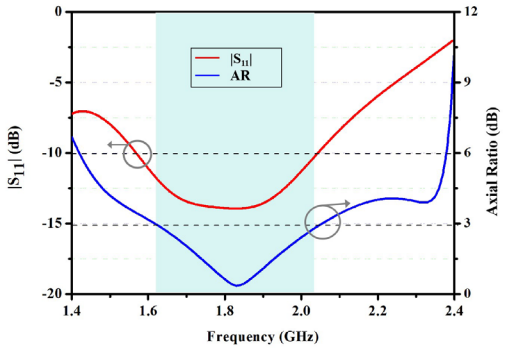

Fig. 3 Simulated $|S_{11}|$ and AR values of the developed wideband CP grid array antenna. The overlapping bandwidth is highlighted in light blue.

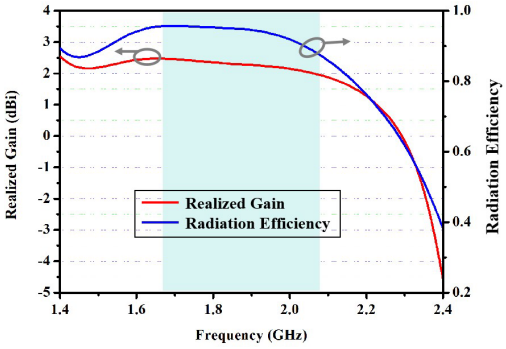

Fig. 4 Simulated realized gain and radiation efficiency values of the developed wideband CP grid array antenna. The overlapping bandwidth is highlighted in light blue.

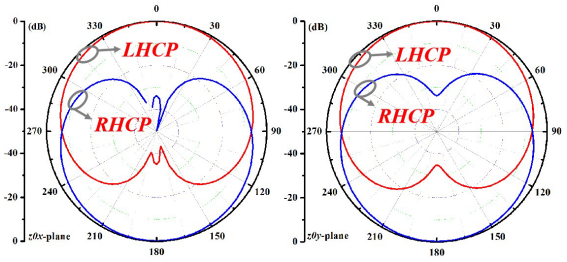

Fig. 5 The normalized realized gain patterns of the developed wideband CP grid array antenna at 1.83 GHz.

IV. CONCLUSION

A compact, wideband, CP antenna was presented in this paper. An inductive grid metasurface structure integrated with a directly drive crossed EAD antenna attained attractive wideband CP radiation performance characteristics. The overlap of the –10-dB impedance bandwidth and the 3-dB AR bandwidth is from 1.67 to 2.06 GHz, a 20.9% fractional bandwidth. This CP antenna radiates a bi-directional electromagnetic wave with symmetric radiation patterns with

high radiation efficiency across the entire overlapping bandwidth. The excellent performance characteristics make it attractive for wideband space-limited wireless communication platforms associated, for example, with global positioning system (GPS), Wi-Fi, and wireless local networks (WLAN) applications.

REFERENCES

[1] S. S. Gao, Q. Luo, and F. Zhu, *Circularly Polarized Antennas*. New York, NY, USA: Wiley, 2013.

[2] J.-W. Baik, T.-H. Lee, S. Pyo, S.-M. Han, J. Jeong, and Y.-S. Kim, "Broadband circularly polarized crossed dipole with parasitic loop resonators and its arrays," *IEEE Trans. Antennas Propag*., vol. 59, no. 1, pp. 80–88, Jan. 2011.

[3] S. X. Ta, K. Lee, I. Park, and R. W. Ziolkowski, "Compact crossed-dipole antennas loaded with near-field resonant parasitic elements," *IEEE Trans. Antennas Propag*., vol. 65, no. 2, pp. 482-488, Feb. 2017.

[4] K. E. Kedze, H. Wang, Y. Kim, and I. Park, "Design of a reduced-size crossed-dipole antenna," *IEEE Trans. Antennas Propag*., vol. 69, no. 2, pp. 689-697, Feb. 2021.

[5] Q. Liu, J. Shen, J. Yin, H. Liu, and Y. Liu, "Compact 0.92/2.45-GHz dual-band directional circularly polarized microstrip antenna for handheld RFID reader applications," *IEEE Trans. Antennas Propag*., vol. 63, no. 9, pp. 3849–3856, Sep. 2015.

[6] Y. Dong, H. Toyao, and T. Itoh, "Compact circularly-polarized patch antenna loaded with metamaterial structures," *IEEE Trans. Antennas Propag.*, vol. 59, no. 11, pp. 4329-4333, Nov. 2011.

[7] Q. Lin, M.-C. Tang, X. Chen, D. Yi, M. Li, and R. W. Ziolkowski, "Low-profile, electrically small, ultra-wideband antenna enabled with an inductive grid array metasurface," *IEEE Trans. Antennas Propag*., early access, Jan. 2022, DOI: 10.1109/TAP.2022.3145459.

[8] M.-C. Tang, Z. Wu, T. Shi, and R. W. Ziolkowski, "Electrically small, low-profile, planar, Huygens dipole antenna with quad-polarization diversity," *IEEE Trans. Antennas Propag.*, vol. 66, no. 12, pp. 6772-6780, Dec. 2018.

[9] M.-C. Tang, Z. Wu, T. Shi, H. Zeng, W. Lin, and R. W. Ziolkowski, "Dual-linearly polarized, electrically small, low-profile, broadside radiating, Huygens dipole antenna," *IEEE Trans. Antennas Propag.*, vol. 66, no. 8, pp. 3877-3885, Aug. 2018.